[CANCER RESEARCH 62, 105–112, January 1, 2002]

Comparative Aflatoxin B_1 Activation and Cytotoxicity in Human Bronchial Cells Expressing Cytochromes P450 1A2 and 3A4[1]

Terry R. Van Vleet, Katherine Macé, and Roger A. Coulombe, Jr.[2]

Graduate Program in Toxicology, Department of Veterinary Sciences, Utah State University, Logan, Utah 84322-4620 [T. R. V. V., R. A. C.], and Nestle Research Centre, Lausanne 26, Switzerland [K. M.]

ABSTRACT

Some epidemiological evidence suggests a link between the inhalation of aflatoxin B_1 (AFB_1)-contaminated grain dusts and increased lung cancer risk. However, the mechanisms of AFB_1 activation and action in human lung are not well understood. We compared AFB_1 action in SV40 immortalized human bronchial epithelial cells (BEAS-2B) with two transfected cell lines that stably express human cytochromes P450 (CYPs) 1A2 (B-CMV1A2) and 3A4 (B3A4), the principal CYPs thought to activate this mycotoxin in human liver. All three cell types retained catalytically active glutathione *S*-transferase, the key phase II enzyme that detoxifies metabolically activated AFB_1. B-CMV1A2 and B3A4 cells expressed methoxyresorufin-*O*-demethylase (MROD) and nifedipine oxidase activities, respectively, and were 3000- and 70-fold more susceptible, respectively, to the cytotoxic effects of AFB_1 than the control cell line (BEAS-2B). When cultured with a range of low, environmentally relevant AFB_1 concentrations (0.02–1.5 μM), control cells formed barely detectable AFB_1-DNA adducts, whereas B-CMV1A2 cells formed significantly more adducts than B3A4 cells. In B-CMV1A2 cells, formation of AFB_1-DNA adducts was inhibited by the CYP 1A2 inhibitor 7,8-benzoflavone, whereas formation of AFB_1-DNA adducts in B3A4 cells was inhibited by the CYP 3A4 inhibitor 17α-ethynylestradiol. Competitive reverse transcription-PCR analysis showed that only the CYP-transfected cell lines expressed CYP mRNA. When adjusted for CYP mRNA expression, B-CMV1A2 cells were more efficient in the formation of cytotoxic and DNA-alkylating species at low AFB_1 concentrations, whereas B3A4 cells were more efficient at high concentrations. Our results affirm the hypothesis that, as in human liver microsomes, CYP 1A2 in human lung cells appears to have a more important role than CYP 3A4 in the bioactivation of low AFB_1 concentrations associated with many human exposures. Therefore, it is possible that under conditions in which appropriate CYPs are expressed in lung, inhalation of AFB_1 may result in increased risk of lung cancer in exposed persons.

INTRODUCTION

AFB_1,[3] a mycotoxin produced by *Aspergillus flavus* and *Aspergillus parasiticus*, is carcinogenic in many animal models and is strongly suspected to be a human carcinogen (1). AFB_1 has been detected in respirable dusts in amounts as high as 52 ppm (2). There is some epidemiological evidence linking pulmonary exposure to AFB_1-laden grain dusts with an increase in lung tumor incidence in certain occupational settings (3). In addition, there is considerable evidence of pulmonary AFB_1 activation in animal models and human and animal tissues (4–8).

Although human CYPs activate AFB_1 to the electrophilic *exo*-AFBO, there is some ambiguity as to which isoform is most important in human liver (9–14). CYPs 1A2 and 3A4 appear to be the most important isoforms for AFB_1 activation in human liver (15), although others (2A6 and 2B7) also activate AFB_1 *in vitro* (16). Both CYPs 1A2 and 3A4, in addition to their mRNA, have been detected in human lung tissues and human lung cells (17). Compared with CYP 3A4, human liver microsomal CYP 1A2 is reported to have a higher affinity toward lower AFB_1 concentrations more reflective of dietary exposures (18). However, CYP 3A4 produces exclusively the *exo*-AFBO, whereas 1A2 also produces equal amounts of the *endo*-AFBO (14). This is important because only *exo*-AFBO is involved in the alkylation of cellular nucleophyles such as DNA. Another complicating component of this issue is the induction of CYPs by exposure to many environmental chemicals (19).

A previous report from this laboratory has shown the potential involvement of CYP 3A4 in AFB_1 activation by human lung tissues at high substrate concentrations (8). Still other studies have shown the role of LOX in human lung AFB_1 activation as well, but very little activation has been seen at concentrations as low as 1.5 μM (7). The role of these various enzymes may be dependent on their magnitude of expression and on the AFB_1 concentration. Less is known about the enzymology of AFBO detoxification in people. In many animals, a key for the detoxification of AFBO is GST-mediated glutathione conjugation (20, 21). Although in humans the M1-1 isoform appears to be the most important isoform *in vitro*, M1-1, M3-3, P1-1, A1-1, and A2-2 GST isoforms can all conjugate the AFBO (20, 22).

The bronchiolar epithelium is the major site of tumor formation in the lung (23). Many cell types are recognized in the bronchiolar epithelium, but there is great variation between species in the cell types present and between the cell types of different species (24–27). BEAS-2B cells are an SV40 immortalized cell line originating from normal human bronchial epithelial cells, which are progenitors of human lung cancer (28), and they have been used as a model for studying human lung cancer (23, 28). They are nontumorigenic and remain so up to very high numbers of passages (28–30). In addition, these cells have been successfully transfected with cDNA for CYPs 1A2 and 3A4 and express stable amounts of these CYPs (15, 23). The CYP-transfected BEAS-2B cell lines used in this study include B-CMV1A2 (transfected with CYP 1A2; Ref. 23) and B3A4 (transfected with CYP 3A4; Ref. 15).

Our laboratory has previously studied AFB_1 metabolism and adduct formation in airways and lung tissues from humans and animals (4–6, 8, 31, 32). The use of animal models is limited for studying the human condition because of variability between species and because human tissues are extremely variable in CYP expression and activities. Here we compare the activation and cytotoxicity of AFB_1 at low concentrations reflective of many human inhalation exposures in human lung cells that stably express CYP 1A2 and 3A4, the two principal isozymes in AFB_1 activation in human liver.

Received 5/8/01; accepted 10/29/01.

The costs of publication of this article were defrayed in part by the payment of page charges. This article must therefore be hereby marked *advertisement* in accordance with 18 U.S.C. Section 1734 solely to indicate this fact.

[1] Supported by NIH-National Institute of Environmental Health Sciences Grant ESO4813, United States Department of Agriculture-National Research Initiative (USDA-NRI) Grants 970-3081 and 980-3754), and the Utah Agricultural Experiment Station, where this paper is designated as number 7384. Portions of this report were presented at the 37th annual meeting of The Society of Toxicology, Seattle, Washington, March 1998 (abstract number 1970).

[2] To whom requests for reprints should be addressed, at Graduate Toxicology Program, Utah State University, 4620 Old Main Hill, Logan, UT 84322-4620. Phone: (435) 797-1598; E-mail: rogerc@cc.usu.edu.

[3] The abbreviations used are: AFB_1, aflatoxin B_1; CYP, cytochrome P450; GST, glutathione *S*-transferase; RT-PCR, reverse transcription-PCR; AFBO, AFB_1-8,9-epoxide; LOX, lipoxygenase; rcRNA, recombinant competitive mRNA; TBS, Tris-buffered saline; PMSF, phenylmethylsulfonyl fluoride; CDNB, chlorodinitrobenzene; MROD, methoxyresorufin-*O*-demethylase.

MATERIALS AND METHODS

Chemicals and Reagents. [^{3}H]AFB_1 (30 Ci/mmol; >98% radiochemical purity) was purchased from Moravek Biochemicals, Inc. (Brea, CA) and diluted with unlabeled AFB_1 to achieve the desired concentrations. LHC-8, epinephrine, and retinoic acid were obtained from Biofluids (Rockville, MD) and used to make LHC-9. LHC Basal and BSA stock were also purchased from Biofluids. Fetal bovine serum was from Hyclone (Logan, UT). Bovine fibronectin, methoxyresorufin, nifedipine, 0.25% trypsin-EDTA, trypsin inhibitor, and Neutral Red solution were purchased from Sigma Chemical Co. (St. Louis, MO). Collagen was a product of Collagen Corp. (Fremont, CA). Resorufin was from Aldrich (Milwaukee, WI), and nitrendipine was from ICN (Irvine, CA). Quickprep Micro mRNA purification kit and First Strand cDNA Synthesis kit were purchased from Amersham (Piscataway, NJ). Riboprobe System T-7 RNA synthesis kit and Taq polymerase were from Promega (Madison, WI). DNA Now reagent was from Biogentex (Seabrook, TX). All custom oligonucleotide primers were purchased from Integrated DNA Technologies (Coralville, IA). 17α-Ethynylestradiol, 7,8-benzoflavone, and all other reagents were purchased from Aldrich.

Culture of BEAS-2B. BEAS-2B cells were cultured with LHC-9 (LHC-8 with 50 ml of 3.3 mM retinoic acid and 250 ml of 0.1% epinephrine) in Corning T_{75} tissue culture flasks (Corning, Corning, NY) at 37°C and 5% CO_2. Cells were passed and harvested using 0.25% trypsin-EDTA and trypsin inhibitor solutions and HBSS (0.9% NaCl and 30 mM HEPES). Flasks were coated with a plate coat (added to flasks 15 min before seeding) consisting of 5 mg of bovine fibronectin, 5 ml of collagen, 50 ml of BSA stock, and 500 ml of LHC Basal.

Quantification of CYP Expression. CYP expression was quantified by competitive quantitative RT-PCR. Poly(A)$^+$ RNA was isolated from B-CMV1A2, B3A4, and BEAS-2B cell types using the Quickprep Micro mRNA purification kit from Amersham. An initial range of mRNA concentrations was amplified by RT-PCR for each cell type to determine the linear range of amplification (0.5–2 ng, B-CMV1A2; 20–150 ng, B3A4; data not shown). An amount of total mRNA in this range was used for competitive quantitative RT-PCR. The primers used for RT-PCR have been described previously (33) and were specific for their target CYP isoform (Table 1). Primers were also designed to span at least one intron to exclude interference from genomic DNA contamination. A modification of the procedure of Vanden Heuvel *et al.* (34) was used to synthesize internal standard rcRNA for each CYP. A DNA template was constructed from the cDNA of each target CYP as filler sequence, which was approximately 60 bp shorter than the target cDNAs (using primers in Table 1). rcRNAs containing competitive primer sequences were synthesized using the Promega T-7 RNA synthesis kit. Next, a range of concentrations (0.1–0.01 ng/50 μl) of rcRNA were added to reaction mixes to compete with target CYP mRNA (within the total cellular mRNA in reaction mixes) to quantify the amount of target mRNA present. The reverse transcription step was performed with the Amersham First Strand cDNA Synthesis kit. First-strand cDNA synthesis mix was diluted to the manufacturer's specifications, and Taq polymerase was added for amplification. The PCR was performed as described previously (35), using the following program: 95°C for 5 min; followed by 27 cycles at 95°C for 30 s, 49°C for 30 s, and 72°C for 1 min, with a 5-min extension at 72°C after the final cycle (Genemate; ISC Bioexpress, Kaysville, UT). Bands were separated electrophoretically on 3% agarose gels (7 × 7.5 × 1 cm) in TAE buffer [0.04 M Tris, 2 mM EDTA, and 0.1% acetic acid (pH = 8.5)] at 200 V for 35 min in a biological cold cabinet (4°C).

CYP Activity Assays. Activity of CYP 1A2 was quantitated by measuring the conversion of methoxyresorufin to resorufin in intact cells as described by Raffali *et al.* (36). T_{75} flasks were seeded at 9.5×10^5 cells/flask and cultured for 96 h to approximately 90% confluence. Growth media were removed and replaced with 5 ml of PBS to wash flasks. After removal of PBS, 2 μM methoxyresorufin containing TBS was added to flasks. Preliminary experiments using a range of concentrations (0–16 μM) showed that 2 μM methoxyresorufin was saturating and therefore not rate-limiting (data not shown). Incubations increasing by 3-min intervals from 0–15 min were determined to be in the linear range for methoxyresorufin conversion to resorufin at 2 μM (data not shown). The TBS-MROD solution was removed, and resorufin production was measured fluorometrically (excitation λ = 530 nm; emission λ = 584 nm; Gilford Flouro IV, San Diego, CA). Resorufin production during the 15-min interval was compared with a resorufin standard curve to quantify resorufin production. Cells were immediately harvested via trypsinization and resuspended in cold storage buffer [0.05 M Tris, 1 mM EDTA, 0.25 M sucrose, 200 μM PMSF, and 20% glycerol (pH 7.4)] before homogenization and storage at −80°C. The protein concentration of this homogenate was determined using the Bradford Protein Microassay (37) and used to calculate the total cellular protein/flask.

Cellular CYP 3A activity was quantitated by nifedipine oxidation, the conditions of which were identical to MROD except for the substrate and its concentration. T_{75} flasks were seeded at 9.5×10^5 cells/flask. After 96 h of culture, flasks were washed with 5 ml of PBS. PBS was replaced with TBS containing 45 μM nifedipine. This concentration of nifedipine was found in preliminary determinations to be within the range of saturation under these conditions (0–55 μM; data not shown). The TBS/nifedipine solution was recovered at 3-min intervals for 15 min, a time interval within the linear phase of product formation (data not shown). Oxidation of nifedipine was analyzed by reverse-phase high-performance liquid chromatography as described previously (Ref. 8; detection limit < 1 nmol). Cells were harvested immediately after TBS/nifedipine removal via trypsinization and suspended in 1 ml of cold storage buffer [0.05 M Tris, 1 mM EDTA, 0.25 M sucrose, 200 μM PMSF, and 20% glycerol (pH 7.4)] before homogenization and storage at −80°C. A 20-μl aliquot of the crude cell homogenate was used for determination of protein concentration by Bradford microassay (37). The amount of total cellular protein/flask was calculated from the results.

Isolation of Cytosol. BEAS-2B, B3A4, and B-CMV1A2 were seeded at 9.5×10^5 cells/T_{75} flask and harvested at 90% confluence (5–6 days later) via trypsinization. The cells were then pelleted and suspended in cold homogenizing buffer [0.05 M Tris, 1 mM EDTA, 0.25 M sucrose, 0.15 M KCl, 20 μM butylated hydroxytoluene, and 200 μM PMSF (pH 7.4)], homogenized, and centrifuged at 600 × *g*. The supernatant was spun again at 10,000 × *g* for 10 min. The resulting supernatant was again centrifuged at 16,000 × *g* for 10 min, and the soluble fraction from this spin was centrifuged at 105,000 × *g* for 1 h. The 105,000 × *g* supernatant (cytosol) was stored at −80°C for later use.

Quantification of GST Activity. GST activity was quantified in the cytosol from each cell type by measuring the rate of conjugation of GST-mediated glutathione to 1 mM CDNB spectrophotometrically (λ = 340 nm; Model DU 640; Beckman, Fullerton, CA) for 10 min at 25°C as described previously (38).

Cytotoxicity Assays. AFB_1 cytotoxicity toward BEAS-2B, B-CMV1A2, and B3A4 cells was determined by the Neutral Red uptake assay (39). For this

Table 1 *Primers used for RT-PCR and rcRNA synthesis*

Primer	Sequence[a]
1A2 forward[b]	TGGCTTCTACATCCCCAAGAAAT
1A2 reverse[b]	TTCATGGTCAGCCCGTAGAT
3A4 forward[b]	CCAAGCTATGCTCTTCACCG
3A4 reverse[b]	TCAGGCTCCACTTACGGT
1A2 rcRNA forward[c]	TAATACGACTCACTATAG*GTGGCTTCTACATCCCCAAGAAAT*TTAACAAGCCCTTGAGTGAG
1A2 rcRNA reverse[c]	TTTTTTTTTTTTTTTTTTT*TTCATGGTCAGCCCGTAGAT*
3A4 rcRNA forward[c]	TAATACGACTCACTATAGG*CCAAGCTATGCTCTTCACCG*ACCCAGAAACTGCATTGGCA
3A4 rcRNA reverse[c]	TTTTTTTTTTTTTTTTTTT*TCAGGCTCCACTTACGGT*

[a] Sequences are oriented 5′ → 3′.
[b] For CYP cDNA synthesis from target mRNA template.
[c] For synthesis of rcRNA template from CYP cDNA. Underline, T7 RNA polymerase promoter sequence incorporated into rcRNA template. *Italics*, competitive sequence incorporated into template for rcRNA synthesis.

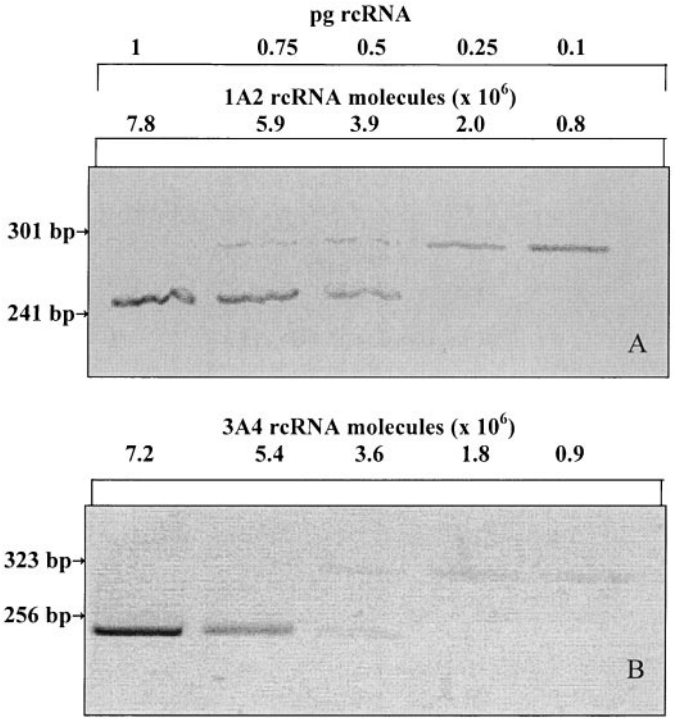

Fig. 1. Reverse image of representative gels from competitive PCR with rcRNA internal standard and target genes for CYP 1A2 (241 and 301 bp, respectively; *A*) and CYP 3A4 (256 and 323 bp, respectively; *B*). The amount of rcRNA spiked into reaction mixes is shown *above* each lane. Wells contained 15 μl of reaction product from competitive quantitative RT-PCR containing either (*A*) 2.5 ng of B-CMV1A2 mRNA or (*B*) 75 ng of B3A4 mRNA and a range of competitor rcRNA (0.1–1 pg). PCR products were resolved on a 3% agarose gel and stained with ethidium bromide.

assay, 96-well plates were seeded at a density of 2.5×10^4 cells/well (in 0.18 ml medium/well). Each plate had a blank and control column. After 24 h of growth, cells were dosed with AFB$_1$, which was serially diluted from the high-dose concentration in subsequent microplate columns, for 24 h (AFB$_1$) or 48 h (7,8-benzoflavone and 17α-ethynylestradiol). After the incubation period, the wells were washed with PBS. Neutral Red media [LHC-9 with Neutral Red (5 mg/ml)] was added, and cells were then incubated for 4 h. Neutral red media were removed, and wells were again washed with PBS before 100 μl of elution buffer (50% ethanol and 1% acetic acid) were added to each well. Plates were shaken for 10 min and read at $\lambda = 540$ nm to measure dye uptake and at $\lambda = 650$ nm for background subtraction. The measured Neutral Red dye uptake was used to calculate the percentage of inhibition of dye uptake as described previously (40) where percentage of inhibition of dye uptake = $[1 - (A_{540}\text{test} - A_{650}\text{test}/A_{540}\text{control} - A_{650}\text{control})] \times 100$. A_{540}test is the spectral absorbance at 540 nm of a test (AFB$_1$) dose group, and A_{650}test is the spectral absorbance of the same test group at 650 nm. A_{540}control is the 540 nm absorbance of the control (no AFB$_1$) wells, and A_{650}test is the 650 nm absorbance of the control group.

Quantitation of AFB$_1$-DNA Adducts. AFB$_1$-DNA adduct formation was quantified as described previously (23). [^{3}H]AFB$_1$ was diluted with cold AFB$_1$, and the specific activity of the stock solution used was 62 μCi/μg AFB$_1$, as determined by liquid scintillation and spectrophotometry ($\lambda = 360$ nm; $\epsilon = 21{,}800$ A/mol AFB$_1$). Cells were seeded at a density of 9.5×10^5 cells/T$_{75}$ flask and cultured 96 h before exposure to [^{3}H]AFB$_1$. Time course studies were performed by exposing cells to 1.5 μM [^{3}H]AFB$_1$ for 2, 4, 8, 16, or 24 h before harvest. Once the optimal incubation time for adduct formation was determined (8 h), subsequent experiments used a range (0.015–15 μM) of AFB$_1$ concentrations. Cultures were harvested via trypsinization, and DNA was isolated from cellular pellets using DNA Now reagent. From the isolated DNA samples 46 μg of genomic DNA were brought to a volume of 1 ml in H_2O and added to 5 ml of scintillation mixture in a 7-ml scintillation vial. The activity of each vial was measured by scintillation counting (Model LS3801; Beckman).

Concentration-Response Modeling and Statistical Analysis. Cytotoxicity plots (percentage of inhibition *versus* μM AFB$_1$) were fit using an empirical three-parameter Hill equation model (41–43):

$$R = \frac{R_{max} \times \text{dose}^n}{K_{0.5}^n + \text{dose}^n}$$

where R is the measured response (percentage of inhibition), $K_{0.5}$ is the AFB$_1$ concentration yielding half of the maximal response (R_{max}), and n is the Hill exponent, which is a measure of cooperativity. An $n = 1$ represents a linear response at low concentrations, an $n > 1$ represents a sublinear (sigmoidal) response indicating cooperativity, and an $n < 1$ represents a supralinear response. The parameters for this equation were calculated using Sigma Plot (Jandel Scientific, San Rafael, CA). Groups were compared for differences using one-way ANOVA (Sigma Chemical Co. Stat Software). A $P < 0.05$ was judged significant.

RESULTS

Using competitive quantitative RT-PCR, we were able to measure the amounts of mRNA specific to each CYP isoform expressed in these cell types. RT-PCR cDNA detection fragments for CYP 1A2 and 3A4 were generated from B-CMV1A2 and B3A4 cells, respectively, using forward and reverse 1A2 or 3A4 primers. DNA templates for recombinant RNA internal standards were constructed using 1A2 or 3A4 rcRNA forward and 1A2 or 3A4 rcRNA reverse primers, and part of each target gene was used as filler sequence. Finally, rcRNAs were synthesized from the DNA templates using the Riboprobe System T-7 RNA synthesis kit. Thus, rcRNAs were as similar as possible to target mRNA in sequence and differed in length by only approximately 60 bp so that PCR products would sufficiently separate by gel electrophoresis.

Fig. 1 clearly shows the predicted PCR products of 241 and 301 bp or 256 and 323 bp from CYP 1A2 and 3A4 rcRNA/mRNA, respectively, generated in this protocol. In each case, the band intensities of products from the rcRNA (241 and 256 bp) decreased as the concentration of spiked rcRNA decreased. Likewise, the band intensities representing PCR products from CYP 1A2 and 3A4 target mRNA (301 and 323 bp, respectively) increased as the PCR product from the rcRNA decreased; the equivalency point between these two products occurred at approximately 0.5 pg of spiked rcRNA competitor. This amount, therefore, represented the amount of target mRNA present in 2.5 and 75 ng of B-CMV1A2 and B3A4 total mRNA, respectively. Using this value, we calculated that B-CMV1A2 cells expressed approximately 5 times more of their respective CYP mRNA than the B3A4 cells (0.37 ± 0.1 amol CYP 1A2 mRNA/ng total mRNA *versus* 0.07 ± 0.02 amol CYP 3A4 mRNA/ng total mRNA, respectively; Fig. 1, *A* and *B*). No CYP 3A4 mRNA was detected in cells other than B3A4, and no CYP 1A2 mRNA was detected in cells other than B-CMV1A2 (data not shown). Furthermore, neither CYP 1A2 nor 3A4 mRNA was detected in BEAS-2B cells (data not shown).

Cellular CYP expression was also assessed by measuring catalytic activities of specific enzyme markers. As expected, activities of MROD and nifedipine oxidase, prototype activities for CYP 1A2 and 3A, respectively, were mainly found in cells that were transfected with cDNA coding for those isozymes. For example, only B-CMV1A2 cells expressed MROD activity, whereas nifedipine oxidase was most significant in B3A4 cells, although small amounts of activity of this enzyme were detected in all cell types (Table 2).

Table 2 *Activities of CYP 1A2 and 3A4 in BEAS-2B, B3A4, and B-CMV1A2 cells*

CYP activities were determined in intact cells as described in "Materials and Methods."

Cell type	MROD[a]	Nifedipine oxidase[a]
BEAS-2B	ND[b]	0.27 ± 0.02[c]
B3A4	ND	4.59 ± 0.66
B-CMV1A2	8.26 ± 0.67	0.33 ± 0.03

[a] nmol mg^{-1} min^{-1} cellular protein.
[b] ND, not detected.
[c] Mean $\pm$ SD ($n = 3$).

Table 3 *GST activity in BEAS-2B, B3A4, and B-CMV1A2 cells*

GST conjugation to CDNB substrate, determined spectrophotometrically, as described in "Materials and Methods."

Cell type	GST activity (nmol/mg min)
BEAS-2B	187 ± 11.5[a]
B3A4	208 ± 11.0
B-CMV1A2	214 ± 19.8

[a] Mean ± SD (n = 4).

Table 4 *Comparative cytoxicity of AFB_1 in BEAS-2B, B3A4, and B-CMV1A2 cells*

		Low [AFB_1]	High [AFB_1]
Cell type	IC_{50}[a]	% Inhibition/CYP[b]	% Inhibition/CYP[c]
BEAS-2B	348 ± 35	ND[d]	ND
B3A4	5.0 ± 0.9	25.7 ± 9.6	959 ± 173
B-CMV1A2	0.11 ± 0.04	164 ± 82	220 ± 79

[a] Mean μM AFB_1 ± SD (n = 4).

[b] Values represent calculated percentage of inhibition of neutral red dye uptake using Hill equation parameters at low AFB_1 concentration (0.25 μM)/amole CYP mRNA/ng total mRNA mean ± SD (n = 4).

[c] Values represent the calculated percentage of inhibition of neutral red dye uptake using Hill equation parameters at a high AFB_1 concentration (10 μM)/amole CYP mRNA/ng total mRNA mean ± SD (n = 4).

[d] ND, not detected.

All cell types retained GST activity, as determined by conjugation to CDNB (Table 3). In addition, CDNB conjugation was not significantly different between the cell types.

Whereas there were consistent AFB_1 concentration-dependent decreases in cell survival, there were profound differences with regard to their sensitivity to AFB_1. B-CMV1A2 cells were by far the most susceptible cell type to AFB_1. B3A4 cells were approximately 70-fold more sensitive to AFB_1 than BEAS-2B cells, whereas B-CMV1A2 cells were roughly 45-fold more sensitive to AFB_1 than cells expressing 3A4 and approximately 3000-fold as sensitive as BEAS-2B cells (Table 4). In each case, regression lines from the percentage of inhibition of dye uptake *versus* AFB_1 concentration curves had good fit for B-CMV1A2 as judged by their r^2 values (Fig. 2, *A*−*C*). The amount of CYP mRNA expressed by each cell type, as determined in competitive RT-PCR, was then used to calculate a ratio of percentage of inhibition:CYP mRNA expressed as a representation of cytotoxicity generated per molecule of CYP mRNA expressed (Fig. 3; low range data are emphasized in the *inset* plot). Thus, on a per molecule mRNA basis, CYP 1A2 was approximately 6-fold more efficient than CYP 3A4 at producing cytotoxic metabolites (in their respective cells) at low (0.25 μM) concentrations (Table 4), and CYP 3A4 was approx-

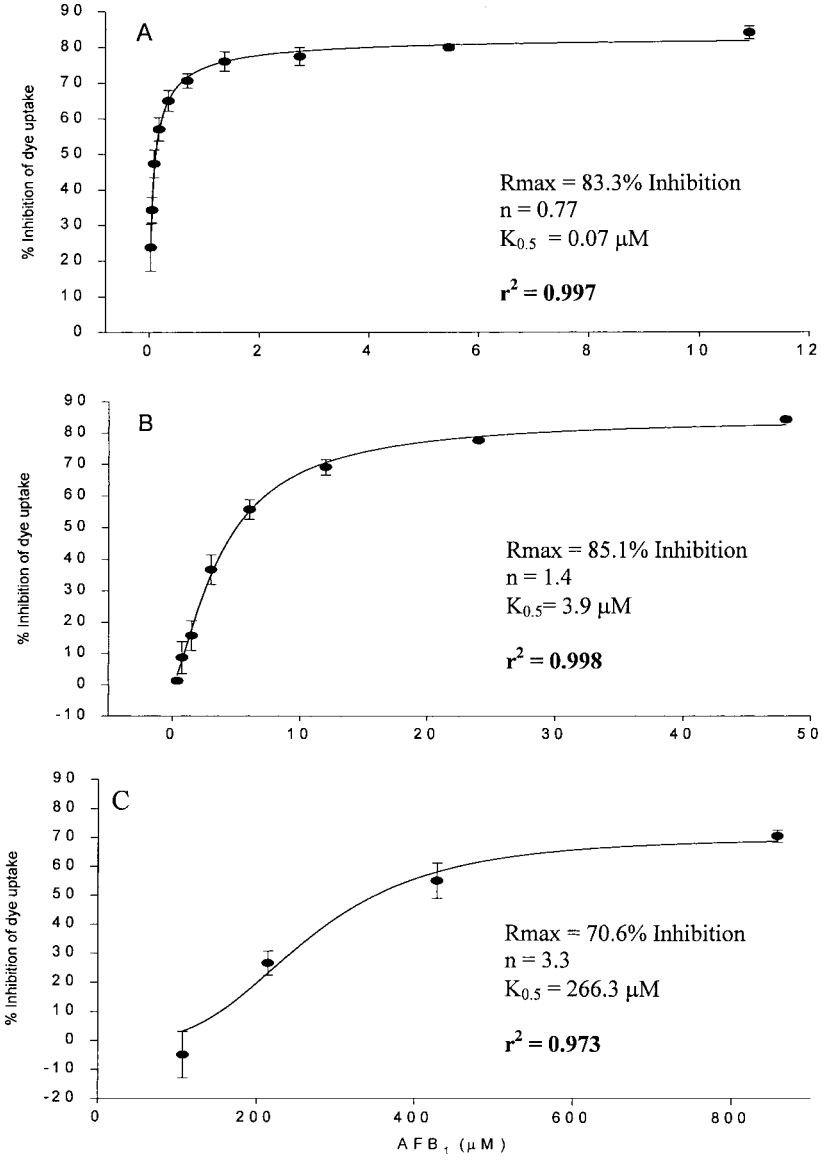

Fig. 2. Comparative AFB_1 cytotoxicity in B-CMV1A2 (*A*), B3A4 (*B*), and BEAS-2B (*C*) cells determined as outlined in "Materials and Methods." Nonlinear regression analysis of this data was used to estimate IC_{50} values of 0.11 μM (B-CMV1A2), 5.0 μM (B3A4), and 348 μM (BEAS-2B), each of which had good fit as judged by high r^2 values. Hill parameters were calculated from the equation: percentage of inhibition = $R_{max}[AFB_1]^n/K^n_{0.5} + [AFB_1]^n$. Data points are mean ± SD (n = 4).

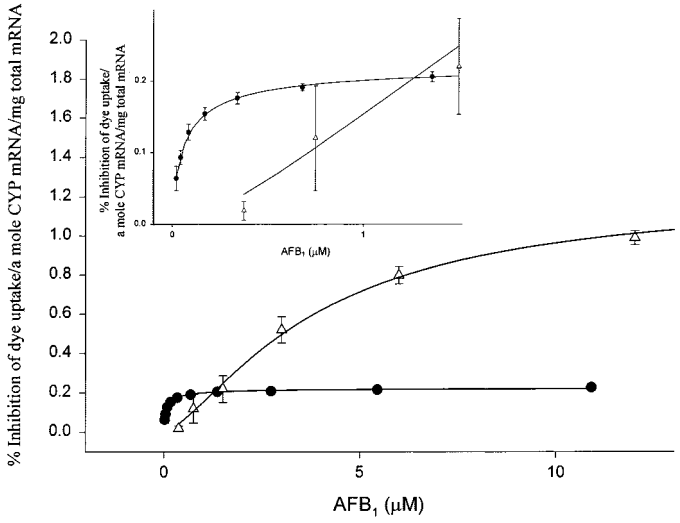

Fig. 3. Cytotoxicity generated by AFB$_1$ in B-CMV1A2 (△) and B3A4 (●) cells as a function of the amount of CYP mRNA expressed. *Inset*, a detail of low-concentration data.

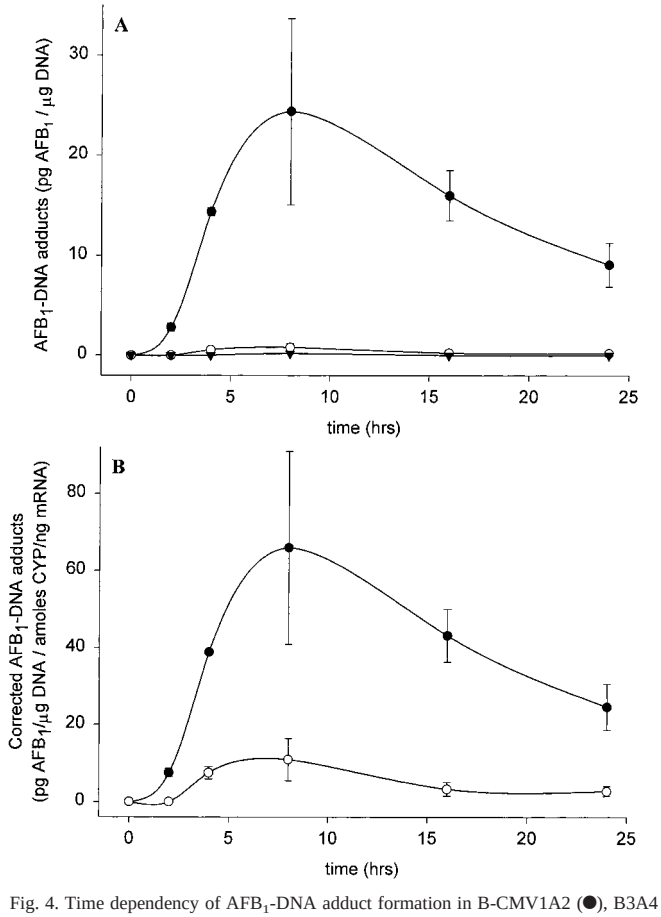

Fig. 4. Time dependency of AFB$_1$-DNA adduct formation in B-CMV1A2 (●), B3A4 (○), and BEAS-2B cells (▼) cultured for up to 24 h in 1.5 μM AFB$_1$ (*A*). AFB$_1$-DNA adduct formation when corrected for the amount of CYP mRNA expressed (*B*). Adduct formation reached peaked at 8 h in both cell types. Data points are the means of duplicate experiments ± range.

imately 5-fold more efficient in this regard at high (10 μM) AFB$_1$ concentrations (Table 4).

Formation of AFB$_1$-DNA adducts is the result of CYP-mediated activation of AFB$_1$ to the reactive AFBO that binds to nuclear DNA. In agreement with the cytotoxicity results, there was a significant difference in the ability of the three cell types to form AFB$_1$-DNA adducts. A preliminary experiment showed that for all cell types, an 8-h incubation time was optimal for AFB$_1$-DNA adduct formation (Fig. 4), a duration that was used in subsequent experiments examining adduct formation over a range of AFB$_1$ concentrations. AFB$_1$-DNA adduct formation was barely detectable in BEAS-2B cells incubated with 0–15 μM AFB$_1$ (Fig. 5). At all concentrations of AFB$_1$ examined, B-CMV1A2 cells bioactivated considerably more AFB$_1$ to DNA-binding species than did B3A4 cells, as evidenced by higher amounts of AFB$_1$-DNA adducts in B-CMV1A2 cells than in B3A4 cells (Fig. 5; data at low concentrations were emphasized in the *inset* plot). This discrepancy between the bioactivation of the two cell types was not as great when corrected for the amount of CYP mRNA expression (Fig. 6; data at low concentrations were emphasized in the *inset* plot). In fact, at higher concentrations of AFB$_1$ (*i.e.*, 8–15 μM), B3A4 cells were more efficient than B-CMV1A2 cells in adduct formation when the amount of CYP mRNA expressed was taken into consideration.

Predictably, the CYP 1A2 inhibitor 7,8-benzoflavone inhibited the formation of AFB$_1$-DNA adducts in B-CMV1A2 cells in a concentration-dependent manner (Fig. 7*A*), whereas adducts in B3A4 cells were inhibited by 17α-ethynylestradiol, a CYP 3A4 inhibitor (Fig. 7*B*). The observed decreases in AFB$_1$ bioactivation caused by 7,8-benzoflavone and 17α-ethynylestradiol were not due to cytotoxicity of these agents at the nanomolar concentrations used in the inhibition assay at the same exposure duration (8 h). These inhibitors were cytotoxic, but only at concentrations several orders of magnitude higher than that found to inhibit AFB$_1$-DNA adduct formation, even when cultured for 48 h (data not shown). At these higher concentrations, 7,8-benzoflavone was significantly more toxic than 17α-ethynylestradiol. A decline in cytotoxicity was observed at higher concentrations (60–120 μM) of 7,8-benzoflavone, resulting from poor solubility of the compound.

DISCUSSION

The biotransformation of AFB$_1$ is a complex process wherein a multitude of CYP isoforms produce several oxidized metabolites of this mycotoxin. In human liver, CYP 1A2 and 3A4 appear to be principal isoforms in AFB$_1$ bioactivation. However, in human lung,

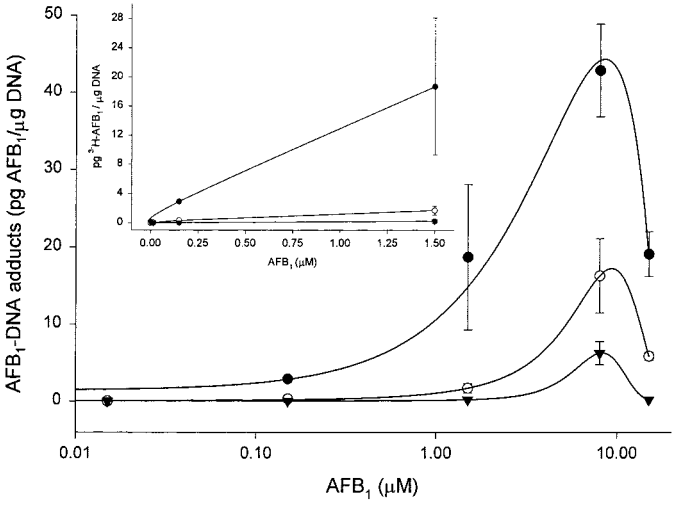

Fig. 5. Effect of AFB$_1$ concentration on formation of AFB$_1$-DNA adducts in B-CMV1A2 (●), B3A4 (○), and BEAS-2B cells (▼). Adduct formation in B-CMV1A2 cells was greatest at every AFB$_1$ concentration examined. *Inset plot* details AFB$_1$-DNA adduct formation at low (0–1.5 μM) AFB$_1$ concentrations. Data points are the means of duplicate experiments ± range.

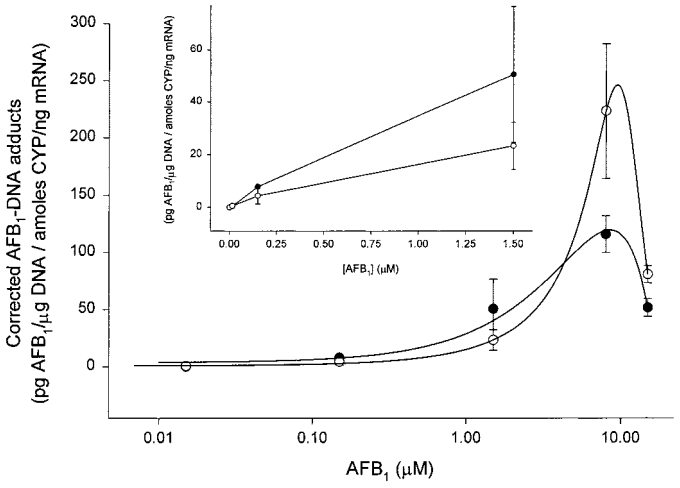

Fig. 6. Formation of AFB$_1$-DNA adducts in B-CMV1A2 (●) and B3A4 (○) over a range of AFB$_1$ concentrations as a function of amount of CYP expressed. These curves show that AFB$_1$-DNA adduct formation predominates at low AFB$_1$ concentrations in B-CMV1A2 cells, whereas that in B3A4 cells predominated at high AFB$_1$ concentrations. *Inset plot* details AFB$_1$-DNA adduct formation at low AFB$_1$ concentrations. Data points are the means of duplicate trials ± range.

the question of which of these isoforms may predominate in bioactivation of AFB$_1$ has not been established. Previous attempts to correlate CYP isoform specificity with respect to AFB$_1$ bioactivation in human lung have often been complicated by interindividual variability and poor stability of phase I enzymes in human lung tissue samples (8). The use of human lung cells that stably express these isoforms potentially overcomes these limitations (23).

Although specific AFB$_1$-DNA adducts were not analyzed in this study, it is possible that the profile of individual adducts is different between the two cell types. For example, in a similar study examining DNA adduct formation and mutations in CYP-expressing human liver cells exposed to AFB$_1$ *in vitro*, Macé *et al.* (9) found that, as in the present study, CYP 1A2-expressing human liver cells were significantly more sensitive to the cytotoxic effects of AFB$_1$ than 3A4-expresing cells. However, the 3A4-expressing cells produced a greater amount of the AFB$_1$-N^7-Gua and ring-opened AFB$_1$-N^7-Fapyr adducts compared with those that express CYP 1A2, which also produced some aflatoxin M$_1$-based DNA adducts (9). Determination of specific AFB$_1$-DNA adducts in these lung cells will be the subject of future investigations.

Competitive RT-PCR was used to measure differences in expression of CYP 1A2 and 3A4 mRNA in the human lung cell types used in this study. This method is highly specific to the isoform being measured (33) and is highly quantitative (34). Importantly, previous studies have shown that 1A2 and 3A4 mRNA levels correlate strongly with their corresponding protein expression and activity (44–46).

Here we report that whereas both CYP 1A2 and 3A4 are capable of bioactivating AFB$_1$, as determined by the ability of cells to produce cytotoxic and genotoxic intermediates, the former isoform appears to be a more predominant contributor at low substrate concentrations. This finding is in agreement with Gallagher *et al.* (47), who demonstrated that CYP 1A2-expressing microsomes likewise predominated in AFB$_1$ activation in human liver compared with those expressing CYP 3A4 at low AFB$_1$ concentrations relevant to many "real world" exposures.

As expected, the transformed cells exhibited CYP activity toward appropriate prototype substrates. For example, the introduction of CYP 3A4 cDNA increased nifedipine oxidase activity, a marker for CYP 3A**,** 15-fold compared with control cells. Likewise, MROD activity, a marker for CYP 1A2, was detected only in the CYP 1A2-expressing B-CMV1A2 cells. Expression of CYP mRNA was specific to transfected cells. In nontransfected BEAS-2B cells, we detected neither CYP 1A2 nor 3A4 mRNA. This is strongly supported by data measuring cytotoxicity, DNA binding, and isoform-specific activity assays. This result is also consistent with a previous report that BEAS-2B cells did not express CYPs 1A2 and 3A4 (48). The lack of CYP expression in this cell line may be a result of immortalization by SV40 large T antigen. It is also possible that the progenitor normal cell(s) for this cell line, which survived SV40 infection to become immortalized, was not a CYP-expressing cell type such as a Clara cell.

All cell types retained GST activity, the key phase II enzyme with respect to AFB$_1$ detoxification. It is also noteworthy that there were no significant differences in GST activity between cell types, suggesting that differences in susceptibility and DNA binding are not due to differences in GST activity but to CYP-mediated activation.

Cytotoxicity is dependent on the enzymatic generation of cytotoxic intermediates. As observed previously (23), introduction of CYP 1A2 and 3A4 cDNA into BEAS-2B cells had a profound effect on the sensitivity of cells in culture toward AFB$_1$. Of the three cell types used in this study, B-CMV1A2 cells were by far the most sensitive to AFB$_1$. B-CMV1A2 cells were 45-fold more susceptible than B3A4 cells and 3000-fold more susceptible than BEAS-2B cells. However, B3A4 cells were 70-fold more susceptible than the nontransformed

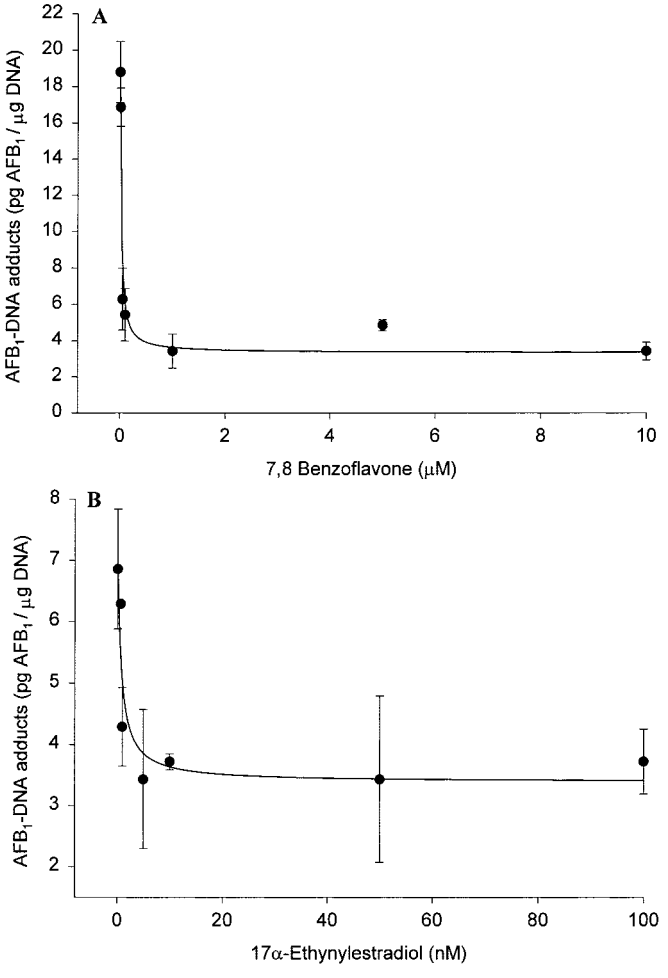

Fig. 7. Effect of CYP inhibitors on the formation of AFB$_1$-DNA adducts in either B-CMV1A2 or B3A4 cells. Inhibition of adduct formation by the CYP 1A2 inhibitor 7,8-benzoflavone in B-CMV1A2 cells (*A*) and effect of the CYP 3A inhibitor 17α-ethynylestradiol inhibition in B3A4 cells (*B*). Cells were exposed with inhibitors and AFB$_1$ concurrently for 8 h as outlined in "Materials and Methods." Data points are the means of duplicate experiments ± range.

BEAS-2B cells. When cytotoxicity was corrected for cellular CYP mRNA expression, CYP 1A2 was approximately 6-fold more efficient than CYP 3A4 in generating cytotoxic intermediates of AFB_1 at low AFB_1 concentrations (Table 4). Our data showing intact B-CMV1A2 cells to be more efficient at bioactivating AFB_1 at low concentrations compared with B3A4 cells supports earlier findings showing that CYP 1A2-expressing microsomes have a higher affinity toward low AFB_1 concentrations than do those expressing CYP 3A4 (10, 18, 49). The Hill constant generated from the AFB_1-mediated cytotoxicity curve in B3A4 cells indicated positive cooperativity (Fig. 2*B*). This observation seems to support previous evidence of two cooperative AFB_1-binding sites in recombinant human liver 3A4 (18, 48).

Formation of AFB_1-DNA adducts, which likewise are dependent on CYP-mediated bioactivation of AFB_1, reflected the comparative susceptibility of these cells to the cytotoxicity of AFB_1. When expressed as a ratio of AFB_1-DNA adducts formed/CYP mRNA expressed, B-CMV1A2 cells were more efficient at activating at low AFB_1 concentrations (0–1.5 μM), whereas B3A4 cells were more efficient at higher concentrations (8–15 μM; Fig. 6). Interestingly, the concentration at which a cross-over of the relative efficiencies of 1A2- and 3A4-expressing cells to mediate AFB_1-DNA adduct formation ($\sim$1.5 μM) occurred was near the point at which a cross-over in the efficiency to generate cytotoxicity also occurred (1–2 μM; Fig. 3).

The profound and specific effect of CYP inhibitors on AFB_1-DNA adduct formation suggests that activation of AFB_1 is primarily due to CYP activity rather than activity by other possible AFB_1-activating enzymes in these cells, such as LOX. LOX has a role in AFB_1 activation in human lung cytosol, but only at relatively high (50 μM) AFB_1 concentrations (7). It may also indicate that CYP-mediated AFB_1 activation may predominate at much lower concentrations.

Whereas CYP 3A4 is commonly isolated in human lung (8, 17, 50, 51), there are conflicting reports regarding whether CYP 1A2 is constitutively expressed. One group of investigators (17) found both CYP 1A2 protein and mRNA in human airway tissues, whereas others did not (8, 50, 52, 53), indicating that this isoform may not be universally expressed or that this protein is particularly unstable. In any event, the expression of this particular isoform is likely to be an important factor in potential risk to inhaled AFB_1.

Any assessment of risk to inhaled AFB_1 should take into account the relative amounts of CYP expression. It is feasible that under conditions where appropriate CYPs are expressed in lung, inhalation of AFB_1 may result in increased risk to lung cancer in exposed persons. Our data indicate that intact human lung cells expressing AFB_1-bioactivating CYP isoforms, especially 1A2, are extremely susceptible to AFB_1, even at low concentrations. It is also important to consider that localized AFB_1 concentrations within human lung cells exposed to AFB_1-laden dusts are largely unknown, making it difficult to accurately predict the *in vivo* roles of CYPs 1A2 and 3A4 for AFB_1 activation in the lung. Additional studies on the relative amounts of pulmonary CYP expression and the range of individual variation of expression will shed more light on the relative roles of these isoforms *in vivo*.

REFERENCES

1. Wong, J. J., and Hsieh, D. P. Mutagenicity of aflatoxins related to their metabolism and carcinogenic potential. Proc. Natl. Acad. Sci. USA, *73:* 2241–2244, 1976.
2. Burg, W. A., Shotwell, O. L., and Saltzman, B. E. Measurements of airborne aflatoxins during the handling of contaminated corn. Am. Ind. Hyg. Assoc. J., *42:* 1–11, 1981.
3. Hayes, R. B., van Nieuwenhuize, J. P., Raatgever, J. W., and Ten Kate, F. J. Aflatoxin exposures in the industrial setting: an epidemiological study of mortality. Food Chem. Toxicol., *22:* 39–43, 1984.
4. Ball, R. W., and Coulombe, R. A., Jr. Comparative biotransformation of aflatoxin B_1 in mammalian airway epithelium. Carcinogenesis (Lond.), *12:* 305–310, 1991.
5. Ball, R. W., Huie, J. M., and Coulombe, R. A., Jr. Comparative activation of aflatoxin B_1 by mammalian pulmonary tissues. Toxicol. Lett., *75:* 119–125, 1995.
6. Coulombe, R. A., Jr., Wilson, D. W., Hsieh, D. P., Plopper, C. G., and Serabjit-Singh, C. J. Metabolism of aflatoxin B_1 in the upper airways of the rabbit: role of the nonciliated tracheal epithelial cell. Cancer Res., *46:* 4091–4096, 1986.
7. Donnelly, P. J., Stewart, R. K., Ali, S. L., Conlan, A. A., Reid, K. R., Petsikas, D., and Massey, T. E. Biotransformation of aflatoxin B_1 in human lung. Carcinogenesis (Lond.), *17:* 2487–2494, 1996.
8. Kelly, J. D., Eaton, D. L., Guengerich, F. P., and Coulombe, R. A., Jr. Aflatoxin B_1 activation in human lung. Toxicol. Appl. Pharmacol., *144:* 88–95, 1997.
9. Mace, K., Aguilar, F., Wang, J. S., Vautravers, P., Gomez-Lechon, M., Gonzalez, F. J., Groopman, J., Harris, C. C., and Pfeifer, A. M. Aflatoxin B_1-induced DNA adduct formation and p53 mutations in CYP450-expressing human liver cell lines. Carcinogenesis (Lond.), *18:* 1291–1297, 1997.
10. Ramsdell, H. S., Parkinson, A., Eddy, A. C., and Eaton, D. L. Bioactivation of aflatoxin B_1 by human liver microsomes: role of cytochrome P450 IIIA enzymes. Toxicol. Appl. Pharmacol., *108:* 436–447, 1991.
11. Shimada, T., and Guengerich, F. P. Evidence for cytochrome P-450NF, the nifedipine oxidase, being the principal enzyme involved in the bioactivation of aflatoxins in human liver. Proc. Natl. Acad. Sci. USA, *86:* 462–465, 1989.
12. Forrester, L. M., Neal, G. E., Judah, D. J., Glancey, M. J., and Wolf, C. R. Evidence for involvement of multiple forms of cytochrome P-450 in aflatoxin B_1 metabolism in human liver. Proc. Natl. Acad. Sci. USA, *87:* 8306–8310, 1990.
13. Raney, K. D., Shimada, T., Kim, D. H., Groopman, J. D., Harris, T. M., and Guengerich, F. P. Oxidation of aflatoxins and sterigmatocystin by human liver microsomes: significance of aflatoxin Q_1 as a detoxication product of aflatoxin B_1. Chem. Res. Toxicol., *5:* 202–210, 1992.
14. Ueng, Y. F., Shimada, T., Yamazaki, H., and Guengerich, F. P. Oxidation of aflatoxin B_1 by bacterial recombinant human cytochrome P450 enzymes. Chem. Res. Toxicol., *8:* 218–225, 1995.
15. Mace, K., Offord, E. A., and Pfeifer, A. M. A. Drug Metabolism and Carcinogen Activation Studies with Human Genetically Engineered Cells. London: Academic Press, 1996.
16. Aoyama, T., Yamano, S., Guzelian, P. S., Gelboin, H. V., and Gonzalez, F. J. Five of 12 forms of vaccinia virus-expressed human hepatic cytochrome P450 metabolically activate aflatoxin B_1. Proc. Natl. Acad. Sci. USA, *87:* 4790–4793, 1990.
17. Mace, K., Bowman, E. D., Vautravers, P., Shields, P. G., Harris, C. C., and Pfeifer, A. M. Characterization of xenobiotic-metabolizing enzyme expression in human bronchial mucosa and peripheral lung tissues. Eur. J. Cancer, *34:* 914–920, 1998.
18. Gallagher, E. P., Kunze, K. L., Stapleton, P. L., and Eaton, D. L. The kinetics of aflatoxin B_1 oxidation by human cDNA-expressed and human liver microsomal cytochromes P450 1A2 and 3A4. Toxicol. Appl. Pharmacol., *141:* 595–606, 1996.
19. Langouet, S., Coles, B., Morel, F., Becquemont, L., Beaune, P., Guengerich, F. P., Ketterer, B., and Guillouzo, A. Inhibition of CYP1A2 and CYP3A4 by oltipraz results in reduction of aflatoxin B_1 metabolism in human hepatocytes in primary culture. Cancer Res., *55:* 5574–5579, 1995.
20. Ketterer, B., Taylor, J., Meyer, D., Pemble, S., Coles, B., Chulin, X., and Spencer, S. Some Functions of Glutathione Transferases. Boca Raton, FL: CRC Press, 1993.
21. Hayes, J. D., Judah, D. J., McLellan, L. I., and Neal, G. E. Contribution of the glutathione *S*-transferases to the mechanisms of resistance to aflatoxin B_1. Pharmacol. Ther., *50:* 443–472, 1991.
22. Johnson, W. W., Ueng, Y. F., Widersten, M., Mannervik, B., Hayes, J. D., Sherratt, P. J., Ketterer, B., and Guengerich, F. P. Conjugation of highly reactive aflatoxin B_1 exo-8,9-epoxide catalyzed by rat and human glutathione transferases: estimation of kinetic parameters. Biochemistry, *36:* 3056–3060, 1997.
23. Mace, K., Gonzalez, F. J., McConnell, I. R., Garner, R. C., Avanti, O., Harris, C. C., and Pfeifer, A. M. Activation of promutagens in a human bronchial epithelial cell line stably expressing human cytochrome P450 1A2. Mol. Carcinog., *11:* 65–73, 1994.
24. McDowell, E. M., Barrett, L. A., Glavin, F., Harris, C. C., and Trump, B. F. The respiratory epithelium. I. Human bronchus. J. Natl. Cancer Inst. (Bethesda), *61:* 539–549, 1978.
25. Plopper, C. G., Mariassy, A. T., Wilson, D. W., Alley, J. L., Nishio, S. J., and Nettesheim, P. Comparison of nonciliated tracheal epithelial cells in six mammalian species: ultrastructure and population densities. Exp. Lung Res., *5:* 281–294, 1983.
26. Plopper, C. G. Comparative morphologic features of bronchiolar epithelial cells. The Clara cell. Am. Rev. Respir. Dis., *128:* S37–S41, 1983.
27. St. George, J. A., Harkema, J. R., Hyde, D. M., and Plopper, C. G. Cell Populations and Structure-Function Relationships of Cells in the Airways. New York: Raven, 1988.
28. Reddel, R. R., Ke, Y., Gerwin, B. I., McMenamin, M. G., Lechner, J. F., Su, R. T., Brash, D. E., Park, J. B., Rhim, J. S., and Harris, C. C. Transformation of human bronchial epithelial cells by infection with SV40 or adenovirus-12 SV40 hybrid virus, or transfection via strontium phosphate coprecipitation with a plasmid containing SV40 early region genes. Cancer Res., *48:* 1904–1909, 1988.
29. Ura, H., Bonfil, R. D., Reich, R., Reddel, R., Pfeifer, A., Harris, C. C., and Klein-Szanto, A. J. Expression of type IV collagenase and procollagen genes and its correlation with the tumorigenic, invasive, and metastatic abilities of oncogene-transformed human bronchial epithelial cells. Cancer Res., *49:* 4615–4621, 1989.
30. Pfeifer, A. M., Jones, R. T., Bowden, P. E., Mann, D., Spillare, E., Klein-Szanto, A. J., Trump, B. F., and Harris, C. C. Human bronchial epithelial cells transformed by the c-raf-1 and c-myc proto-oncogenes induce multidifferentiated carcinomas in nude mice: a model for lung carcinogenesis. Cancer Res., *51:* 3793–3801, 1991.
31. Wilson, D. W., Ball, R. W., and Coulombe, R. A., Jr. Comparative action of aflatoxin B_1 in mammalian airway epithelium. Cancer Res., *50:* 2493–2498, 1990.

32. Ball, R. W., Wilson, D. W., and Coulombe, R. A., Jr. Comparative formation and removal of aflatoxin B_1-DNA adducts in cultured mammalian tracheal epithelium. Cancer Res., *50:* 4918–4922, 1990.
33. Hakkola, J., Pasanen, M., Purkunen, R., Saarikoski, S., Pelkonen, O., Maenpaa, J., Rane, A., and Raunio, H. Expression of xenobiotic-metabolizing cytochrome P450 forms in human adult and fetal liver. Biochem. Pharmacol., *48:* 59–64, 1994.
34. Vanden Heuvel, J. P., Tyson, F. L., and Bell, D. A. Construction of recombinant RNA templates for use as internal standards in quantitative RT-PCR. Biotechniques, *14:* 395–398, 1993.
35. Finnstrom, N., Bjelfman, C., Thorn, M., Loof, L., and Rane, A. Quantitation of cytochrome P450 mRNAs in patients with suspected liver diseases as assessed by reverse transcriptase-polymerase chain reaction. J. Lab. Clin. Med., *134:* 133–140, 1999.
36. Raffali, F., Rougier, A., and Roguet, R. Measurement and modulation of cytochrome-P450-dependent enzyme activity in cultured human keratinocytes. Skin Pharmacol., *7:* 345–354, 1994.
37. Bradford, M. M. A rapid and sensitive method for the quantitation of microgram quantities of protein utilizing the principle of protein-dye binding. Anal. Biochem., *72:* 248–254, 1976.
38. Habig, W. H., Pabst, M. J., and Jakoby W. B. Glutathione *S*-transferases. The first enzymatic step in mercapturic acid formation. J. Biol. Chem., *249:* 7130–7139, 1974.
39. Fautz, R., Husein, B., and Hechenberger, C. Application of the neutral red assay (NR assay) to monolayer cultures of primary hepatocytes: rapid colorimetric viability determination for the unscheduled DNA synthesis test (UDS). Mutat. Res., *253:* 173–179, 1991.
40. Dombrink-Kurtzman, M. A., Bennett, G. A., and Richard, J. L. An optimized MTT bioassay for determination of cytotoxicity of fumonisins in turkey lymphocytes. J. AOAC Int., *77:* 512–516, 1994.
41. Melnick, R. L., Kohn, M. C., Dunnick, J. K., and Leininger, J. R. Regenerative hyperplasia is not required for liver tumor induction in female B6C3F1 mice exposed to trihalomethanes. Toxicol. Appl. Pharmacol., *148:* 137–147, 1998.
42. Jenski, L. J., and Kleyle, R. M. Kinetic assay of cytotoxic T lymphocyte clones. I. Methodology and data analysis. J. Immunol. Methods, *117:* 181–190, 1989.
43. Jenski, L. J. Kinetic assay of cytotoxic T lymphocyte clones. II. Comparison of primary and secondary responses and lectin-dependent cytotoxicity. J. Immunol. Methods, *117:* 191–198, 1989.
44. Seree, E. J., Pisano, P. J., Placidi, M., Rahmani, R., and Barra, Y. A. Identification of the human and animal hepatic cytochromes P450 involved in clonazepam metabolism. Fundam. Clin. Pharmacol., *7:* 69–75, 1993.
45. Sumida, A., Kinoshita, K., Fukuda, T., Matsuda, H., Yamamoto, I., Inaba, T., and Azuma, J. Relationship between mRNA levels quantified by reverse transcription-competitive PCR and metabolic activity of CYP3A4 and CYP2E1 in human liver. Biochem. Biophys. Res. Commun., *262:* 499–503, 1999.
46. George, J., Liddle, C., Murray, M., Byth, K., and Farrell, G. C. Pre-translational regulation of cytochrome P450 genes is responsible for disease-specific changes of individual P450 enzymes among patients with cirrhosis. Biochem. Pharmacol., *49:* 873–881, 1995.
47. Gallagher, E. P., Wienkers, L. C., Stapleton, P. L., Kunze, K. L., and Eaton, D. L. Role of human microsomal and human complementary DNA-expressed cytochromes P4501A2 and P4503A4 in the bioactivation of aflatoxin B_1. Cancer Res., *54:* 101–108, 1994.
48. Offord, E. A., Mace, K., Ruffieux, C., Malnoe, A., and Pfeifer, A. M. Rosemary components inhibit benzo[*a*]pyrene-induced genotoxicity in human bronchial cells. Carcinogenesis (Lond.), *16:* 2057–2062, 1995.
49. Crespi, C. L., Penman, B. W., Steimel, D. T., Gelboin, H. V., and Gonzalez, F. J. The development of a human cell line stably expressing human CYP3A4: role in the metabolic activation of aflatoxin B_1 and comparison to CYP1A2 and CYP2A3. Carcinogenesis (Lond.), *12:* 355–359, 1991.
50. Raunio, H., Hakkola, J., Hukkanen, J., Pelkonen, O., Edwards, R., Boobis, A., and Anttila, S. Expression of xenobiotic-metabolizing cytochrome P450s in human pulmonary tissues. Arch. Toxicol. Suppl., *20:* 465–469, 1998.
51. Raunio, H., Hakkola, J., Hukkanen, J., Lassila, A., Paivarinta, K., Pelkonen, O., Anttila, S., Piipari, R., Boobis, A., and Edwards, R. J. Expression of xenobiotic-metabolizing CYPs in human pulmonary tissue. Exp. Toxicol. Pathol., *51:* 412–417, 1999.
52. Hukkanen, J., Lassila, A., Paivarinta, K., Valanne, S., Sarpo, S., Hakkola, J., Pelkonen, O., and Raunio, H. Induction and regulation of xenobiotic-metabolizing cytochrome P450s in the human A549 lung adenocarcinoma cell line. Am. J. Respir. Cell Mol. Biol., *22:* 360–366, 2000.
53. Shimada, T., Yun, C. H., Yamazaki, H., Gautier, J. C., Beaune, P. H., and Guengerich, F. P. Characterization of human lung microsomal cytochrome P-450 1A1 and its role in the oxidation of chemical carcinogens. Mol. Pharmacol., *41:* 856–864, 1992.